

# The TPL-Lambda Gripper: A Tendon-Driven Manipulator for Combined Pinching and Lifting Based on the Scott Linkage

Shijie Qu

School of Artificial Intelligence, Shenzhen Tech. Univ.

Lab of Robotics, X-Institute, Shenzhen, China

[gushijie644@gmail.com](mailto:gushijie644@gmail.com)

Wenzeng Zhang\*

Lab of Robotics, X-Institute, Shenzhen, China

Dept. of Mechanical Engineering, Tsinghua Univ., Beijing, China

[wenzeng75@163.com](mailto:wenzeng75@163.com)

\*Co-corresponding author

Che Zhang\*

School of Artificial Intelligence, Shenzhen Tech. Univ.

Shenzhen, China

[zhangche@sztu.edu.cn](mailto:zhangche@sztu.edu.cn)

\*Corresponding author

**Abstract**—In modern industrial settings, parts are often stored in fixtures or trays, creating localized "embedded constraints" such as grooves, clips, or steps. These constraints frequently cause traditional pick-and-place grasping to fail due to environmental interference. To address this, we propose a novel grasp strategy: Lift-Then-Operate (LTO). The key idea is that after two fingers achieve a parallel pinch grasp, they lift the object along a near-vertical straight-line trajectory to dislodge it, creating free space for subsequent transfer or assembly operations. To implement this strategy, we designed the TPL-Lambda, a single-actuator underactuated gripper. It utilizes a Scott linkage to generate the required vertical trajectory at the fingertip, combined with a parallelogram structure to maintain fingertip orientation. A single motor and tendon drive simultaneously achieve grasping and the retracting/lifting motion. Experimental results demonstrate that the TPL-Lambda can robustly lift objects such as motors, shafts, and small parts, effectively overcoming embedded constraints. This work simplifies the concept of "designing fingertip force vectors to overcome environmental constraints" into a single-DOF vertical lifting strategy, offering both theoretical clarity and engineering practicality.

**Keywords**—*Scott linkage, Lift-Then-Operate, underactuated gripper, Tendon-driven mechanism, adaptive grasping, mechanism design component.*

## I. INTRODUCTION

In industrial settings, parts are usually neatly placed in fixtures or trays to ensure accurate positioning and batch processing. However, such placement often creates local "embedded constraints," such as V-shaped grooves, limit edges, elastic clips, or step structures. These constraints make conventional "in-place grasping" methods prone to failure due to environmental interference [1]. In contrast, the human hand can naturally interact with its environment in such scenarios — for example, sliding along a support surface to contact a target or adjusting the grasping posture when encountering obstacles [2]. Most robotic grippers, however, are still designed under the idealized assumption of free-space grasping [3], making it difficult to achieve stable grasps when dealing with thin, small, or embedded parts.

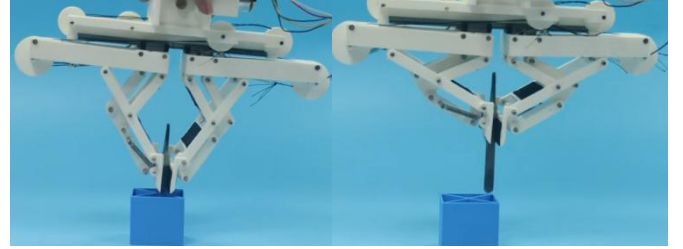


Fig. 1. Concept of the LTO strategy and the TPL-Lambda gripper. After a parallel pinch grasp, the object is lifted vertically to disengage it from embedded constraints, creating free space for subsequent manipulation.

To address this problem, researchers have proposed various underactuated and adaptive robotic hand designs. Underactuated mechanisms exploit the coupling of a small number of actuators with elastic elements, enabling fingers to achieve shape adaptation without complex control [4]. Birglen [5] developed kinematic and static models of underactuated fingers, while the Dollar SDM hand [6] highlighted the importance of compliance in adaptive grasping. Subsequent studies introduced the Coupled and Self-Adaptive (COSA) mode [7] and developed hybrid hands such as COSA-E and CDSA [8].

In addition, Chen [9] proposed the LPCSA hand, capable of both linear-parallel pinching and coupled self-adaptation, and Feng [10] investigated the adaptive performance of multi-DOF underactuated fingers. These works have greatly expanded the design space for underactuated grasping.

Nevertheless, most adaptive grasping research still focuses on modeling multi-point contact between objects and fingers, with limited consideration of environmental constraints [11]. In practice, parts are often placed on tables or embedded in slots, where rigid fingertips may collide with the environment and cause grasping failure. Babin and Gosselin [12] proposed a passive joint gripper with an epicyclic gear, enabling2 fingertip bending through table sliding for scooping actions, though its adaptability was limited to planar surfaces.

Similarly, Lévesque [13] introduced a model-based scooping gripper optimized for smooth surfaces, but its generalization to complex environments remained limited.

This work was supported by Natural Science Foundation of Top Talent of SZTU (grant no. GDRC202334).

Research supported by the Foundation of Enhanced Student Research Training (E-SRT) and Open Research for Innovation Challenges (ORIC), X-Institute.

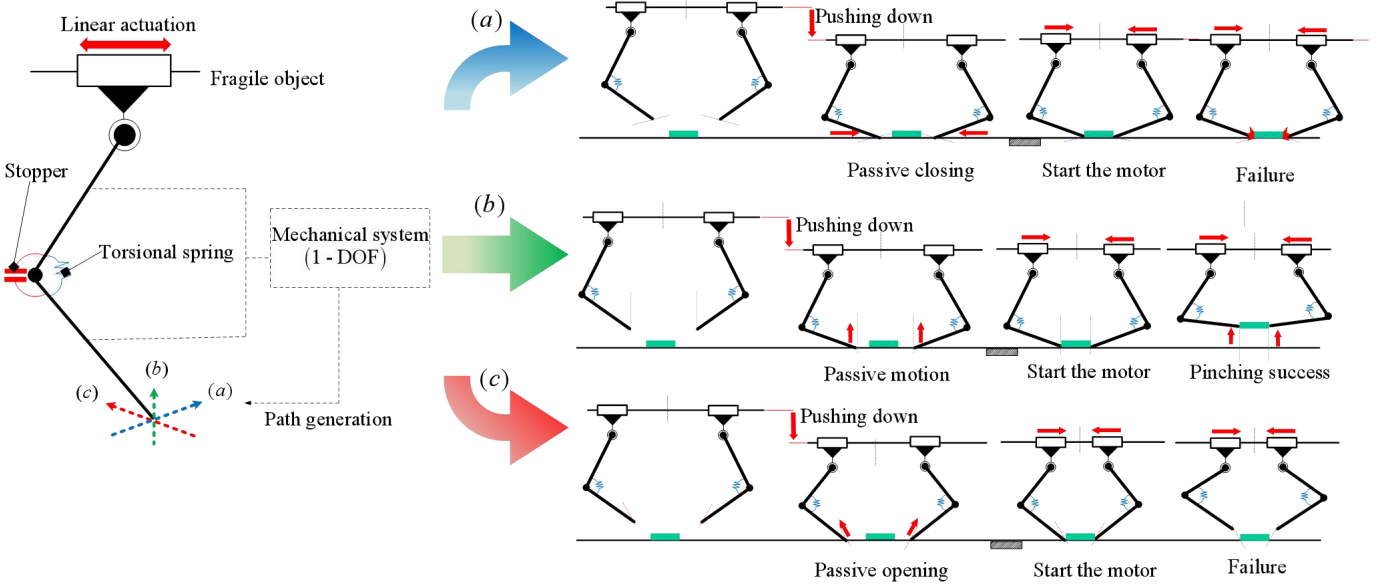


Fig. 2. Comparison of different fingertip straight-line trajectories during grasping and lifting. (a) Inward-tilted trajectory; (b) Vertical straight-line trajectory; (c) Outward-tilted trajectory.

To overcome these challenges, some studies have adopted the idea of “exploiting the environment” in gripper design. Eppner [1] argued that effective grippers should leverage physical contacts and environmental constraints to handle uncertainty during manipulation, which has inspired the development of “physical intelligence” hands.

Yoon is OMEGA hand [14] combined Hart's linkage with a parallelogram, allowing fingertip bending when interacting with tabletops and showing potential to overcome obstacles such as steps or slopes. However, the fingertip trajectory lacked experimental validation, and the complex linkage structure—with many parts and high manufacturing cost—limited its applicability in real-world engineering.

Meanwhile, other teams have developed specialized structures and compliant mechanisms. Cha [15] and Mak [16] achieved rapid scooping of thin objects through high-speed motion and controlled compliance; He [17] adopted spoon-shaped jaws with pneumatic actuation to grasp and transfer food; and Ko [18] proposed a tendon-driven gripper with switchable underactuated surfaces, enabling both in-hand manipulation and object transport. In competitions, suction and electrostatic adhesion have also been widely applied. For example, in the Amazon Picking Challenge, many teams used suction-based or angled sheet-like grippers to handle thin objects [19]. Despite their effectiveness, suction often fails on rough or porous surfaces, while electrostatic adhesion is restricted by material types.

Overall, existing methods still show clear limitations in stable grasping under environmental constraints. Soft hands offer excellent compliance but often suffer from limited gripping force, dynamic response, and control complexity. Rigid underactuated hands, while advantageous in structure

and cost, lack effective integration of environmental interaction mechanisms. Therefore, enabling vertical compliance and environmental adaptability, while maintaining basic functions such as parallel pinching, has become a key challenge.

To this end, this paper introduces a new grasping strategy called “Lift-Then-Operate (LTO).” Under this strategy, the gripper first establishes a parallel pinch grasp and then lifts the object vertically to disengage it from constraints. The freed workspace allows subsequent operations such as flipping, insertion, or precise alignment. This concept is consistent with the research on “designing fingertip force vectors to overcome environmental constraints”[20], but is simplified into a single-DOF vertical lifting motion, making it easier to integrate with linear actuators and more practical for engineering applications.

To realize this strategy, we designed the TPL-Lambda gripper based on the Scott linkage. The design integrates a parallelogram structure with elastic elements, enabling vertical compliance of fingertips after pinching, and allows both pinching and lifting to be achieved with a single motor. Based on a mechanical model, we conducted prototype experiments to validate the gripper is robustness in lifting motors, shafts, and small parts. This study provides a new approach for grasping tasks under environmental constraints in industrial settings and extends the design framework of underactuated robotic hands.

The remainder of this paper is organized as follows: Section I introduces the background; Section II explains the operating principle of vertical lifting; Section III describes the structure of the proposed gripper; Section IV presents the mechanical analysis under actuation conditions; Section V reports experimental results with the prototype; and Section VI concludes with a summary and outlook.

## II. ANALYSIS AND SELECTION OF LIFTING TRAJECTORIES

Figure 2 illustrates four stages of grasping when the robotic arm and actuator work in coordination, with the gripper following different straight-line trajectories at various angles. The sequence is as follows: the robotic arm first drives the

Trajectory (a): An inward-tilted path. This trajectory can provide greater gripping force and a certain degree of self-locking during grasping. However, during subsequent motion, it is prone to interference from the environment, making it unsuitable for stable in-hand manipulation.

Trajectory (b): A vertical straight-line trajectory. The fingertip motion is perpendicular to the table surface, avoiding both excessive increase and loss of gripping force. As a result, it enables stable lifting after grasping. This trajectory is therefore adopted in this study as the target fingertip path.

Trajectory (c): If the fingertip continues along this trajectory after grasping, without external motion compensation, gripping failure and object dropping are likely to occur, leading to unsuccessful operations.

Based on the above analysis, we select the vertical straight-line trajectory as the target path for the fingertip's linear-generating mechanism. In the following sections, the gripper prototype will be designed and implemented with the Scott linkage as its core.

## III. MECHANICAL STRUCTURE DESIGN OF THE GRIPPER

To achieve the vertical straight-line trajectory of the fingertip shown in Fig. 2, this study adopts the Scott linkage as the core structure. The geometric condition of this mechanism is as follows: when  $AB = BC = BD$ , point  $B$  lies on a chord of a circle centered at  $A$  with radius  $r$ , and the angle between  $CB$  and  $AB$  is  $90^\circ$ , point  $C$  generates a vertical straight-line trajectory (Fig. 3).

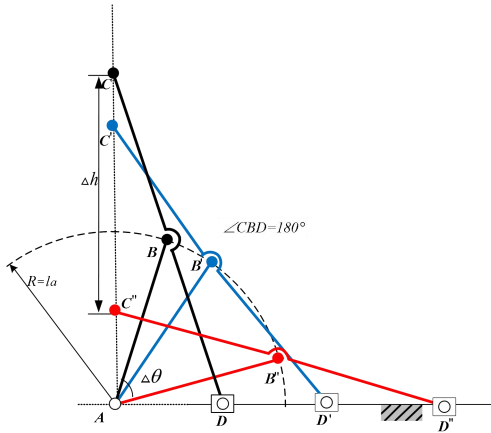


Fig. 3. Principle of the Scott linkage

Based on this principle, we developed a compound robotic gripper capable of both parallel pinching and lifting operations, named the TPL-Lambda gripper (Tendon-Driven Pinching and Lifting Gripper). The name derives from the geometry of the Scott linkage, which resembles the Greek letter “λ.” The structure and functions are introduced as follows.

gripper downward; after contacting the table surface, a parallel pinch is executed; then, under actuator drive, the fingertips move the object along the predetermined trajectory.

Three representative trajectories are considered:

### A. Finger Mechanism

Figure 3 shows the relationship between  $\Delta h$  and  $\Delta\theta$  when the Scott linkage is in vertical motion.

We define the linkage parameters as follows:  $l_{AB}$ ,  $l_{CB}$  and  $l_{AD}$  represent the length of the first finger segment, the second finger segment and the distance between the origin and the slide rail respectively.  $l_{CD}$  is the drive linkage, which enables the tip point  $C$  to move precisely along a straight line. The relationships among the parameters of these linkages can be obtained through formulas, so as to better set the initial state of the fingers and enable the fingers to better respond to external forces.

The mechanical characteristics of the Scott linkage itself are:

$$l_{CB} = l_{AB} = l_{BD} \quad (1)$$

In the initial state,  $l_{AD}$  satisfies the following relationship:

$$l_{AD} = 2l_{AB}\cos\angle BAD \quad (2)$$

The distance  $l_{AC}$  from the distal joint axis to the finger base satisfies:

$$l_{AC} = 2l_{AB}\sin\angle BAD \quad (3)$$

Set the length of the first finger segment as previously determined  $l_{AB} = 50\text{mm}$ ,  $\angle BAD = 70^\circ$ , The corresponding values of  $l_{AD} = 34.2\text{ mm}$  and  $l_{AC} = 93.97\text{ mm}$ , along with  $l_{AB}$ ,  $l_{AD}$ ,  $l_{AC}$ ,  $l_{CD}$  and angle  $\angle BAD$ , are stored in Table 1.

TABLE I. DIMENSION PARAMETERS OF THE TPL-LAMBDA FINGER

Predetermined parameters			Designed parameters	
$l_{AB}$	$l_{CD}$	$\angle BAD$	$l_{AC}$	$l_{AD}$
50 mm	10 mm	$70^\circ$	93.97 mm	34.2 mm

Based on the Scott linkage, we further integrated a parallelogram mechanism, torsional spring, stopper, tendon, and pulley to build a complete finger structure (Figs. 4 and 5):

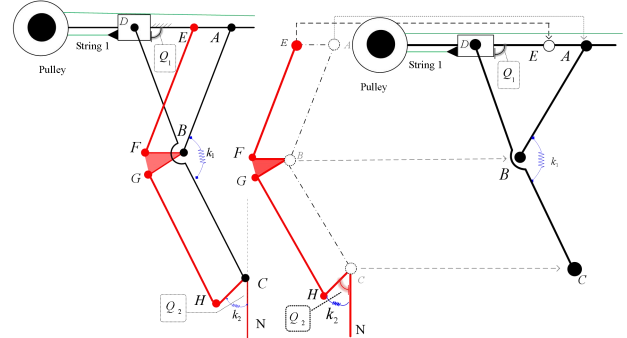


Fig. 4. Structural design of the TPL-Lambda finger

A torsional spring  $k_1$  is installed at joint  $B$ , enabling the finger to reset automatically after bending and enhancing adaptability to environmental constraints; A stopper is placed at the initial position of the slider to ensure accurate reset after interaction; A winding drum is mounted at the base to guide tendon actuator. The tendon is fixed to the slider. The motor drives the slider retraction via the winding drum, lifting the fingertip vertically and achieving the compound motion from pinching to lifting.

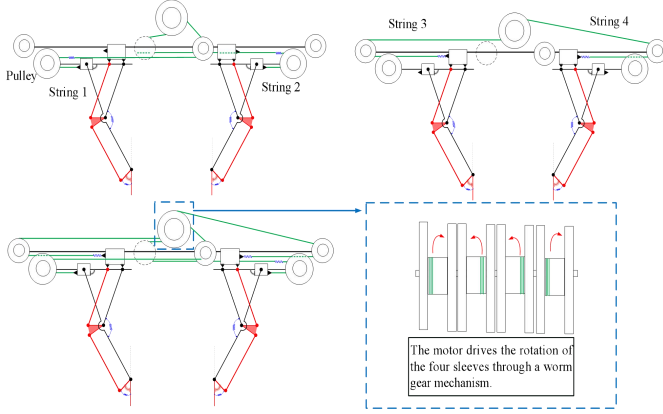


Fig. 5. Tendon transmission path of the TPL-Lambda finger

#### A. Functional Implementation of the TPL-Lambda.

##### a. Environmental Interaction

As shown in Fig. 4, the Scott and parallelogram mechanisms share joints  $A$ ,  $B$ , and  $C$ . This improves structural compactness and leverages the stability of the parallelogram in planar pinching, enabling reliable object grasping with two fingers. Moreover, the vertical compliance of the fingertips allows passive adaptation to contact forces during pinching (Fig. 6).

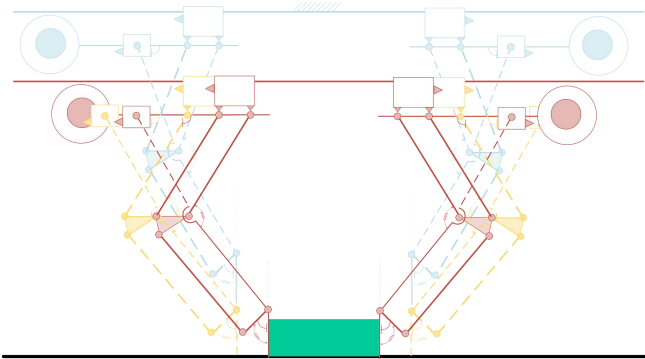


Fig. 6. Passive compliance of the TPL-Lambda during environmental interaction

##### b. Lifting Operation

The lifting function is realized through two tendon-driven stages (Fig. 7):

1. Pinching stage: the motor pulls the tendon to close the gripper, completing parallel pinching of the object.

2. Lifting stage: after pinching, the motor continues pulling, causing the slider to retract and the fingertip to move vertically upward, thereby disengaging the object from constraints.

Ideally, the maximum lifting distance equals the length of  $AC$ . In practice, the lifting stroke can be adjusted by mechanical stoppers. To ensure reliable disengagement, the stroke should be greater than the theoretical value with an additional safety margin.

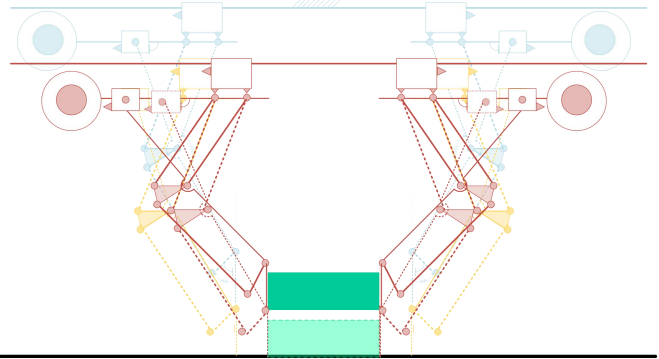


Fig. 7. Lifting operation stages of the TPL-Lambda.

In summary, the TPL-Lambda gripper combines the Scott linkage with a parallelogram mechanism, achieving both stable parallel pinching and active vertical lifting. Its adaptive design enhances grasping stability and environmental adaptability, providing an effective solution for handling constrained objects in industrial environments.

## IV. FORCE ANALYSIS

#### A. Introduction

In our experiments, it was observed that grasping performance is closely related to factors such as tendon selection, motor drive capability, drum diameter, stiffness of the parallelogram structure, and the stiffness of the torsion spring at joint  $B$ . These factors directly influence the fingertip output force and the motor's lifting capability. Therefore, we must systematically analyze their mechanisms of action and establish design criteria through the modeling of the transmission chain.

This section focuses on the mechanical modeling and theoretical derivation of the transmission chain: motor torque, tendon tension, slider thrust, fingertip vertical force, load and anti-slip constraints. The primary objectives are: (I) to determine the minimum motor torque required for the lifting phase; (II) to calculate the maximum mass that can be lifted for a given torque; and (III) to establish the anti-slip conditions during the gripping phase. To facilitate the derivation, the coefficient  $n_s$  is introduced to represent the number of effective tendon segments on the drum (e.g.,  $n_s = 2$  for a symmetric dual-branch configuration,  $n_s = 1$  for a single-branch).

The analysis employs a quasi-static assumption: the inertia of the links and the weight of the tendons are neglected; the springs  $k_1$  and  $k_2$  are treated as equivalent additional forces without altering the main transmission topology; losses from the tendon path, guide pulleys, and slides are incorporated into

an equivalent efficiency  $\eta_p$ . The coordinate system is defined as follows: the vertical upward direction is  $+y$ , and the gripper closing direction is  $+x$ . The definitions and geometric relationships of the relevant physical quantities are illustrated in Fig. 8.

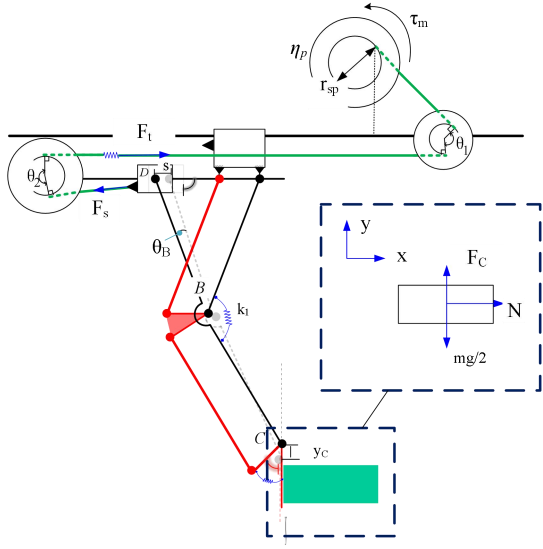


Fig. 8. Force Diagram

### B. Torque to Fingertip Force Mapping

The kinematic relationship between the displacement  $s$  of the slider  $D$  and the vertical displacement  $y_c$  of the fingertip  $C$  is defined by the Jacobian  $J(s)$ :

$$J(s) = \frac{\partial y_c}{\partial s} \quad (4)$$

The motor torque  $\tau_m$  is converted into the total tendon tension  $F_t$  on the drum with radius  $r_{sp}$ :

$$F_t = \frac{\tau_m}{n_s r_{sp}} \quad (5)$$

Considering the transmission efficiency  $\eta_p$ , the effective thrust force  $F_s$  applied to the slider is:

$$F_s = \eta_p F_t = \eta_p \frac{\tau_m}{n_s r_{sp}} \quad (6)$$

Applying the principle of virtual work for the system:

$$F_s \delta s = F_c \delta y_c \quad (7)$$

The mechanical advantage  $M_a(s)$ , defined as the ratio of output force to input force, is derived from Eqs. (6) and (7) and is the reciprocal of the Jacobian:

$$M_a(s) = \frac{F_c}{F_s} = \frac{1}{J(s)} \quad (8)$$

Substituting Eqs. (5) and (6) into Eq. (8) yields the expression for the vertical lifting force  $F_c(s)$  at the fingertip as a function of motor torque:

$$F_c(s) = \frac{\eta_p}{n_s r_{sp}} \frac{\tau_m}{J(s)} \quad (9)$$

For the straight-line segment of the SR mechanism where  $J(s) \approx 1$ . The variations of  $y_c(s)$  and the mechanical advantage  $M_a(s)$  are illustrated in Fig. 9.

### C. Lifting Criteria: Minimum Torque and Maximum Mass

For a stable lift of a mass  $m$  with a safety factor  $(1+\gamma)$ , the vertical force provided by a single fingertip must satisfy:

$$F_c \geq \frac{mg}{2}(1+\gamma) \quad (10)$$

Substituting the expression for  $F_c(s)$  from Eq. (9) into Eq. (10) yields the minimum motor torque required at a specific slider position  $s$ :

$$\tau_m^{\min}(s) = \frac{mg}{2}(1+\gamma) \frac{n_s r_{sp} J(s)}{\eta_p} \quad (11)$$

Conversely, the maximum mass  $m_{\max}^{(r)}$  that can be lifted for a given motor torque  $\tau_m$  is:

$$m_{\max}^{(r)} = \frac{2\eta_p \tau_m}{n_s r_{sp} J(s) g} s \quad (12)$$

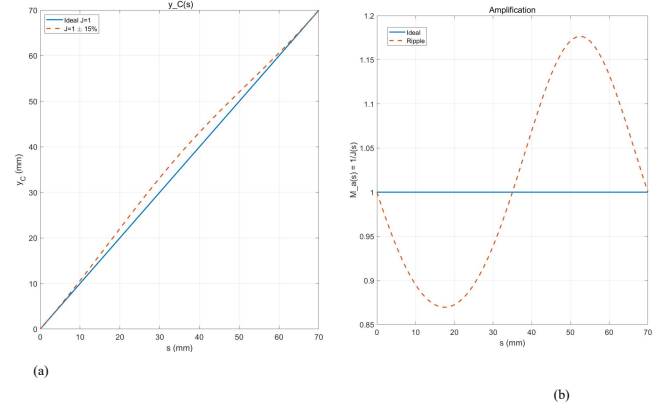


Fig. 9. Relationship between fingertip displacement  $y_{C(s)}$  and mechanical advantage  $M_a(s)$

Expressing the motor torque in terms of power  $P$  and angular velocity  $\omega$  ( $P=\tau_m \omega$ ), the maximum mass under constant-speed operation is given by:

$$m_{\max}^{(P)} = \frac{2\eta_p P}{n_s r_{sp} J(s) g \omega} \quad (13)$$

The relationship between  $\tau_m^{\min}$  and  $m$ , described by Eq. (11), is represented by a family of curves in Fig. 10, providing a direct design tool for motor selection or load capacity estimation.

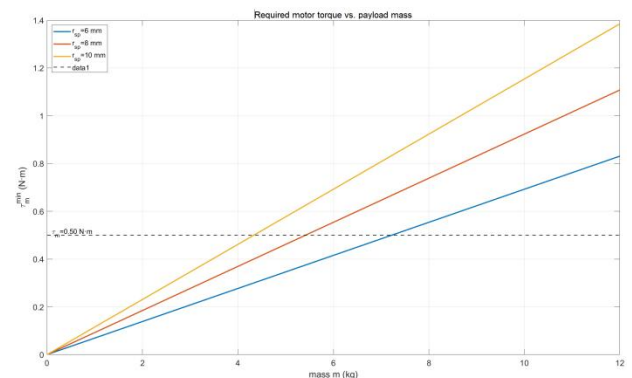


Fig. 10. Family of curves: Minimum required motor torque  $\tau_m^{\min}$  vs. mass  $m$

#### D. Anti-Slip Condition during Grasping

During the grasping phase prior to lifting, the normal force  $N$  must provide sufficient static friction to prevent slip. The anti-slip condition for one fingertip is:

$$\frac{mg}{2} \leq \mu_f N \Rightarrow N \geq \frac{mg}{2\mu_f} \quad (14)$$

This normal force  $N$  is typically generated by a dedicated linear actuator (e.g., a lead screw). The relationship between the torque  $\tau_e$  of this actuator and the resulting thrust force  $F_e$  is approximately:

$$F_e \approx \frac{2\pi\eta_e}{p} \tau_e, \quad N = \alpha F_e \quad (15)$$

where  $p$  is the screw pitch,  $\eta_e$  is the efficiency, and  $\alpha$  is a mechanical advantage factor relating the thrust to the generated normal force at the fingertip.

#### V. GRASPING EXPERIMENTS

To validate the underactuated gripper design concept based on the TPL-Lambda mechanism proposed in this paper, a prototype was designed and manufactured. A series of grasping experiments were conducted to systematically evaluate its functional performance, environmental interaction capability, and load-bearing capacity. This section details the design and fabrication process of the prototype and demonstrates its experimental performance in various scenarios, thereby proving the effectiveness and robustness of the design.

##### A. Design and Fabrication of the Prototype

The 3D model of the gripper prototype was designed using SolidWorks software, considering structural rationality, kinematic coordination, and printing feasibility. All structural components were fabricated using Fused Deposition Modeling (FDM) 3D printing technology. Polylactic Acid (PLA) was selected as the primary material due to its excellent printability, sufficient structural strength, and low cost, achieving an optimal balance between cost-effectiveness and functional requirements during the prototype development stage. The manufactured prototype is shown on Fig. 11.

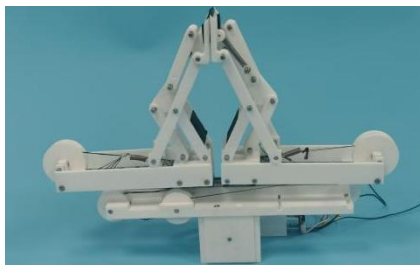


Fig. 11. Figure 11. Overall design of the TPL-Lambda gripper

To enhance grasping stability and interaction performance, a special design was implemented on the contact surface between the TPL-Lambda fingertip and the object: a 2mm deep fingertip groove was designed. A textured silicone sheet

of matching thickness (2mm) was adhered inside the groove to optimize the surface interaction between the fingertip and the object. Compared to the exposed PLA material surface, the textured silicone sheet significantly provides a higher coefficient of friction, making the grasping process more stable and the lifting experimental results more pronounced. Meanwhile, the flexibility and elasticity of the silicone material allow it to better adapt to minor irregularities on the object's surface and buffer contact impacts, thus more realistically simulating the compliant mechanical properties of human fingertips, aligning with the concept of soft grasping. The motion process and overall structure of the designed gripper under no-load conditions are shown in Fig. 12, clearly demonstrating its continuous and smooth trajectory from opening to closing.

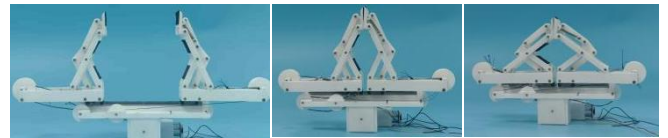


Fig. 12. The continuous motion trajectory of the TPL-Lambda gripper under no-load conditions.

##### B. Validation of Environmental Interaction and Anti-Interference Capability

An excellent gripper must not only stably grasp target objects but also possess strong environmental interaction capabilities—that is, it should not be overly sensitive to accidental contact with the environment and should even maintain a stable grip or continue functioning normally after experiencing certain disturbances.

To validate this performance of the prototype, targeted experiments were conducted. As shown in Fig. 13, during the gripping operation, the outer side of the gripper's fingers was actively made to collide with a rigid desktop surface. The experimental results demonstrate that the prototype exhibits outstanding anti-interference capability against environmental disturbances.

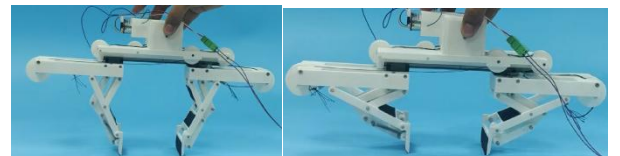


Fig. 13. Collision test between the gripper finger and a rigid desktop, validating its environmental interaction and anti-interference capability

##### A. Lifting Performance Tests

Lifting capacity is a key metric for evaluating gripper performance, as it directly tests the gripper's ability to apply a vertical upward force after grasping an object and stably lift it. Two types of lifting experiments were designed to comprehensively assess the performance of the prototype.

First, we tested its ability to grasp and lift small everyday objects on a desktop. As shown in Fig. 14a, the gripper

adapted to small objects of different shapes, successfully applying sufficient normal and frictional forces to overcome gravity and achieve stable lifting. This demonstrates the reliability of its fundamental grasping functionality.

Second, a more challenging test was conducted—grasping and lifting heavier objects "embedded" in the environment. As shown in Fig. 14b, the target objects included a motor placed inside a box, tweezers, and a soldering iron inserted into a base. This scenario simulates common industrial operations, such as extracting components from tightly confined spaces. During the lifting process, the gripping force was evenly distributed, exhibiting no slippage or object tilting, fully replicating the delicate human-like "pinch-and-lift" operation.

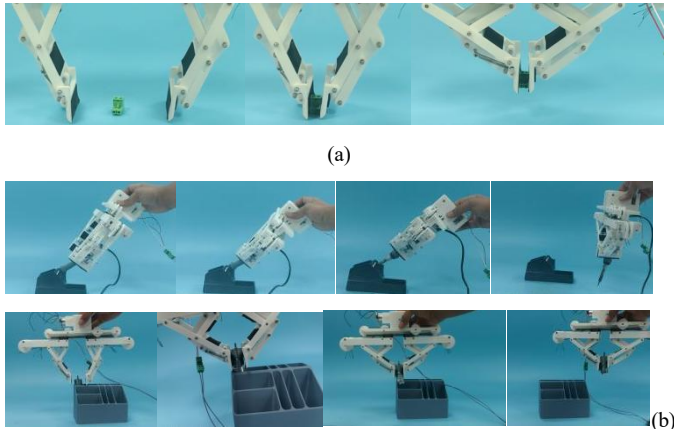


Fig. 14. (a) Lifting small objects on a flat surface; (b) Lifting embedded objects from constrained spaces.

Additionally, the prototype demonstrated versatile capabilities in reliably grasping objects of various shapes.

## VI. CONCLUSIONS

This paper presented a novel approach to grasping objects within embedded environmental constraints, common in industrial fixtures and kitting. We introduced the Lift-Then-Operate (LTO) paradigm, which decouples the grasping process into a reliable parallel pinch followed by a vertical lifting motion to disengage the object, before any subsequent manipulation. This strategy effectively circumvents the limitations of traditional static grasping in confined spaces.

To realize this strategy, we designed the TPL-Lambda gripper, an underactuated, single-DOF mechanism. Its core innovation lies in the integration of a Scott linkage to generate a near-vertical lifting path, coupled with a parallelogram structure to maintain stable fingertip orientation. A single tendon actuator seamlessly drives both the grasping and lifting phases, enhancing simplicity and reliability.

Through theoretical analysis and prototype experiments, we validated the gripper's key functionalities: its ability to interact compliantly with surfaces during approach and grasp, and its capacity to successfully lift a variety of objects (including motors, shafts, and small components) from their complex environmental adaptation can be achieved through mechanical intelligence and a well-designed kinematic

structure, reducing reliance on complex control or additional sensors. In summary, this work provides a practical and mechanistically elegant solution to a persistent challenge in robotic grasping. The LTO strategy and the TPL-Lambda design offer a new perspective for end-effector design, emphasizing the exploitation of controlled motion sequences rather than just static grasp geometry.

## REFERENCES

- [1] C. Eppner, R. Deimel, J. Álvarez-Ruiz, et al., "Exploitation of environmental constraints in human and robotic grasping," *Int. J. Robot. Res.*, vol. 34, no. 7, pp. 1021–1038, 2015.
- [2] W. Jia, A. Ramirez-Serrano, Y. Liu, "Real-Time Interactive Capabilities of Dual-Arm Systems for Humanoid Robots in Unstructured Environments," in *Proc. IEEE Int. Conf. Autom. Sci. Eng. (CASE)*, Bari, Italy, pp. 474–481, Aug. 2024.
- [3] Y. Kageyama, M. Hamaya, K. Tanaka, et al., "Learning Scooping Deformable Plastic Objects Using Tactile Sensors," in *Proc. IEEE Int. Conf. Autom. Sci. Eng. (CASE)*, Bari, Italy, pp. 4020–4025, Aug. 2024.
- [4] T. Laliberté and C. M. Gosselin, "Simulation and design of underactuated mechanical hands," *Mech. Mach. Theory*, vol. 33, no. 1–2, pp. 39–57, 1998.
- [5] L. Birglen and C. M. Gosselin, "Kinetostatic analysis of underactuated fingers," *IEEE Trans. Robot. Autom.*, vol. 20, no. 2, pp. 211–221, 2004.
- [6] A. M. Dollar and R. D. Howe, "The SDM hand as a prosthetic terminal device: A feasibility study," in *Proc. IEEE 10th Int. Conf. Rehabil. Robot.*, pp. 978–983, 2007.
- [7] G. Li and W. Zhang, "Study on coupled and self-adaptive finger for robot hand with parallel rack and belt mechanisms," in *Proc. IEEE Int. Conf. Robot. Biomimetics (ROBIO)*, pp. 1110–1115, 2010.
- [8] D. Liang, W. Zhang, X. Xu, "COSA-E hand: A coupled and self-adaptive hand with eccentric wheel mechanisms," in *Proc. IEEE Int. Conf. Robot. Biomimetics (ROBIO)*, Qingdao, China, pp. 544–549, Dec. 2016.
- [9] S. Chen, B. Zhang, K. Feng, Y. Wang, J. Li, and W. Zhang, "A Novel Geometrical Structure Robot Hand for Linear-Parallel Pinching and Coupled Self-Adaptive Hybrid Grasping," in *Proc. IEEE/RSJ Int. Conf. Intell. Robots Syst. (IROS)*, Abu Dhabi, UAE, pp. 3030–3036, Oct. 2024.
- [10] K. Feng, Z. Duan, C. Han, Z. Guo, W. Zhang, "Underactuated finger topology for humanoid robot grasp," in *Proc. IEEE Int. Conf. Adv. Robot. Mechatron. (ICARM)*, Qingdao, China, Jul., pp. 753–758, 2024.
- [11] L. U. Odhner, R. R. Ma, A. M. Dollar, "Open-Loop Precision Grasping with Underactuated Hands Inspired by a Human Manipulation Strategy," *IEEE Trans. Autom. Sci. Eng.*, vol. 10, no. 3, pp. 2830–2835, Jul. 2013.
- [12] V. Babin, D. St-Onge, C. Gosselin, et al., "Stable and Repeatable Grasping of Flat Objects on Hard Surfaces Using Passive and Epicyclic Mechanisms," *Robot. Comput. Integrat. Manuf.*, vol. 55, pp. 1–10, 2019.
- [13] F. Lévesque, B. Sauvet, P. Cardou, et al., "A Model-Based Scooping Grasp for the Autonomous Picking of Unknown Objects with a Two-Fingered Gripper," *Robot. Auton. Syst.*, vol. 106, pp. 14–25, 2018.
- [14] D. Yoon, K. Kim, "Fully Passive Robotic Finger for Human-Inspired Adaptive Grasping in Environmental Constraints," *IEEE/ASME Trans. Mechatronics*, vol. 27, no. 5, pp. 3841–3852, 2022.
- [15] H. Cha, I. Lee, and J. Seo, "High-Speed Scooping Through Dynamic Manipulation: Model and Practice," *IEEE Robot. Autom. Lett.*, vol. 10, no. 2, pp. 1377–1384, 2025.
- [16] K. H. Mak, J. Seo, "High-Speed Scooping Manipulation Using Controlled Compliance," in *RSS Workshop on High-Speed Robotics*, London, UK, pp. 10261–10267, 2022.
- [17] T. He, S. Aslam, Z. Tong, et al., "Scooping Manipulation via Motion Control with a Two-Fingered Gripper and Its Application to Bin Picking," *IEEE Robot. Autom. Lett.*, vol. 6, no. 4, pp. 6394–6401, Oct. 2021.
- [18] T. Ko, "A Tendon-Driven Robot Gripper with Passively Switchable Underactuated Surface and Its Physics Simulation-Based Parameter Optimization," *IEEE Robot. Autom. Lett.*, vol. 5, no. 4, pp. 5002–5009, 2020.
- [19] N. Correll, K. E. Bekris, D. Berenson, et al., "Analysis and Observations from the First Amazon Picking Challenge," *IEEE Trans. Autom. Sci. Eng.*, vol. 15, no. 1, pp. 172–188, Jan. 2018.
- [20] D. Yoon and K. Choi, "Analysis of Fingertip Force Vector for Pinch-Lifting Gripper with Robust Adaptation to Environments," *IEEE Trans. Robot.*, vol. 39, no. 5, pp. 3501–3515, Oct. 2023.